Preparation and Characterization of Poly(vinylidene fluoride)/Sulfonated Poly(phthalazinone ether sulfone ketone) Blends for Proton Exchange Membrane

Shuang Gu, Gaohong He, Xuemei Wu, Zhengwen Hu, Leilei Wang, Gongkui Xiao, Lin Peng

State Key Laboratory of Fine Chemicals, R&D Center of Membrane Science and Technology, Dalian University of Technology, Dalian, Province of Liaoning, China 116012, China

Received 22 November 2008; accepted 3 October 2009
DOI 10.1002/app.31547
Published online 10 December 2009 in Wiley InterScience (www.interscience.wiley.com).

ABSTRACT: Poly(vinylidene fluoride)/sulfonated poly (phthalazinone ether sulfone ketone) (PVdF/SPPESK) blend membranes are successfully prepared by solution blending method for novel proton exchange membrane (PEM). PVdF crystallinity, FTIR-ATR spectroscopy, thermal stability, morphology, water uptake, dimension stability, and proton conductivity are investigated on PVdF/SPPESK blends with different PVdF contents. XRD and DSC analysis reveal that the PVdF crystallinity in the blends depends on PVdF content. The FTIR-ATR spectra indicate that SPPESK remains proton-conducting function in the blends due to the intactness of $-SO_3H$ group. Thermal analysis results show a very high thermal stability (T_{d1} = 246–261°C) of the blends. PVdF crystallinity and morphology study demonstrate that with lower PVdF content, PVdF are very compatible with SPPESK. Also, with lower PVdF content, PVdF/SPPESK blends possess high water uptake, e.g., P/S 10/90 and P/S 15/85 have water uptake of 135 and 99% at 95°C, respectively. The blend membranes also have good dimension stability because the swelling ratios are at a fairly low level (e.g., 8–22%, 80°C). PVdF/SPPESK blends with low PVdF content exhibit very high proton conductivity, e.g., at 80°C, P/S 15/85 and P/S 10/90 reach 2.6×10^{-2} and 3.6×10^{-2} S cm^{-1}, respectively, which are close to or even higher than that (3.4×10^{-2} S cm^{-1}) of Nafion115 under the same test condition. All above properties indicate that the PVdF/SPPESK blend membranes (particularly, with 10–20% of PVdF content) are very promising for use in PEM field.
 J Appl Polym Sci 116: 852–860, 2010

Key words: proton exchange membrane; sulfonated poly(phthalazinone ether sulfone ketone); poly(vinylidene fluoride); blend; fuel cell

INTRODUCTION

Proton exchange membranes (PEMs) have received considerable attention as membrane electrolytes in both proton exchange membrane fuel cells (PEMFCs)[1] and direct methanol fuel cells (DMFCs).[2] Up to now, perfluorosulfonic polymer membranes, represented by DuPont's Nafion, have been widely used due to the high proton-conductivity, high electrochemical/chemical stability, and excellent mechanical strength. Despite those favorable properties, still Nafion suffers a few drawbacks, such as high cost, low thermal stability, and high methanol permeability. These limitations have stimulated many efforts in developing alternative PEMs. The direct/indirect sulfonation on thermostable aromatic polymers is the typical route to prepare the novel PEMs, because the sulfonated polymers not only are proton-conductive, but also have low cost, high thermal stability, and high resistance of methanol permeation. Owing to the low acidity of aromatic sulfonic acid ($-Ar-SO_3H$) in these sulfonated polymers compared with that of perfluorosulfonic acid ($-CF_2-SO_3H$) in Nafion, their proton conductivity is significantly limited when having same/similar ion exchange capacity (IEC). High IEC is demandingly required to obtain high conductivity, but excessively high IEC can result in extreme swelling of membranes, i.e., loss of dimension stability. Therefore, sulfonated polymers with varying sulfonic acid concentration have the tradeoff between high conductivity and good dimension stability.[3] As a result, these sulfonated polymers are still difficult to be used in practice.

To solve this problem, some techniques such as pore filling,[4] acid–base ionic crosslinking,[5–7] and covalent

Correspondence to: G. He (hgaohong@dlut.edu.cn).
Contract grant sponsor: National Natural Science Foundation of China; contract grant number: 50273005.
Contract grant sponsor: Program for New Century Excellent Talents in Chinese Universities, the Education Ministry of China; contract grant number: NCET-06-0272.
Contract grant sponsor: Scientific Research Foundation for the Returned Overseas Chinese Scholars (State Education Ministry of China).

crosslinking have been developed.[8–11] Unfortunately, the loss of conductive material is still of concern in the pore-filling membranes because of the weak interaction between the conductive material and porous substrate. The acid–base ionically crosslinked membranes usually suffer the worse stability at elevated temperatures (e.g., 70–80°C), due to collapse of the interaction between acid and base groups. Also most of covalently crosslinked membranes suffer severe brittleness, because the covalent crosslinking can enormously restrict rotation and movement of polymer chains. On the other hand, the polymer blending is another potential approach to avoid the above disadvantages of the three techniques mentioned. Polymer blend consists of both a hydrophilic sulfonated polymer to provide proton conductivity and a hydrophobic polymer to provide flexibility and dimension stability.

Poly(vinylidene fluoride) (PVdF) has strong hydrophobicity, good mechanical strength, sufficient chemical stability, and high dimension stability. PVdF has been used widely in the battery[12–14] and also in PEM field. For example, PVdF was radiation-grafted and subsequently sulfonated for radiation-grated PEMs[15–17]; or soaked with inorganic acids (e.g., H_2SO_4 or H_3PO_4)[18–21] for doping PEMs. More importantly, due to the excellent compatibility to form blend pairs with various hydrophilic polymers containing oxygen atom,[22] PVdF was also used to prepare the blend PEMs with sulfonic acid group containing polymers, e.g., Nafion,[23–26] sulfonated polystyrene (SPS),[27–30] sulfonated styrene-divinylbenzene copolymer [SP (St-DVB)],[31,32] sulfonated styrene-(ethylene-butylene)-styrene block coplymer (SEBS),[33] and sulfonated poly(ether ether ketone) (SPEEK).[34–36] These PVdF/sulfonated polymer blend membranes exhibited favorable properties such as enhanced dimension stability and reduced methanol permeability.

Poly(phthalazinone ether sulfone ketone) (PPESK) is one of the most promising thermostable aromatic polymers as matrix for PEM. The corresponding pristine sulfonated PPESK (SPPESK)[37–39] and covalently-crosslinked SPPESK for PEM have been reported[40] previously. These SPPESK-based PEMs exhibited high thermal stability, low methanol permeability, and comparable conductivity. However, little attention has been focused on the blending of PVdF and SPPESK for PEM. In this work, the PVdF/SPPESK blend membranes have been prepared and PVdF crystallinity, FTIR-ATR spectroscopy, thermal stability, morphology, water uptake, dimension stability, and proton conductivity of the blend membranes with different PVdF contents were investigated.

EXPERIMENTAL

Materials and chemicals

PPESK with a sulfone/ketone unit-ratio of 1 : 1 (S/K = 1/1) was provided generously by Prof. Dr. Jian in Dalian University of Technology. PVdF (average M_w = 750,000) was purchased from Shanghai Jing De Kang Co. (Shanghai, China). Sulfuric acid (96–98%), fuming sulfuric acid (20–23% SO_3), dimethylacetamide (DMAc), acetone, 1-methyl-2-pyrrolidone (NMP), and other chemicals were obtained commercially and used without further purification.

Synthesis and separation of SPPESK

SPPESK with 106% of degree of sulfonation (DS) is carefully selected to blend with PVdF in the study, since the blend membranes not only have good resistance in hot water, but also possess high IEC. SPPESK (DS: 106%, IEC: 2.04 mmol g^{-1}) was synthesized by sulfonating PPESK with the mixture of sulfuric acid and fuming sulfuric acid (volume ratio of 1 : 1, and the corresponding concentration of the mixture, C_{H2SO4}, of 100.77%) at 60°C for 2 h. Separation and purification of SPPESK were carried out by an organic solvent reprecipitation method. The detailed synthesis and separation procedures were reported in our previous work.[38] Chemical structures of SPPESK and PVdF were shown in Scheme 1.

Preparation of PVdF/SPPESK blend membranes

PVdF and SPPESK (DS: 106%) were dissolved individually in NMP (10 wt %), then the two solutions were mixed uniformly at the given mass ratios. The solution-mixture was cast on a glass plate, and the PVdF/SPPESK blend membranes were obtained after curing and drying at 60°C for 4 days. For convenience, PVdF/SPPESK blend membranes with mass ratios of from 5/95 to 50/50 are denoted as from P/S 5/95 to P/S 50/50 correspondingly.

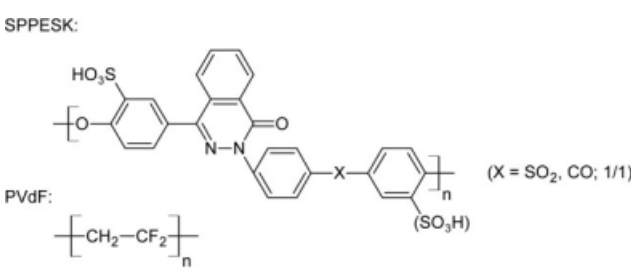

Scheme 1 Chemical structures of SPPESK and PVdF.

X-ray diffraction (XRD) and differential scanning calorimetry (DSC)

XRD analysis was performed to disclose the crystalline structures of the membranes using a D/MAX 2400 diffractometer. The wavelength of the X-ray is 1.5418 Å (Cu-K α radiation) at a wide range of Bragg ranges (2θ: 4–60°). The scanning rate is 6° min^{-1} and the resolution is 0.01°. DSC technique was used to measure PVdF crystallinity by a Mettler Toledo DSC 821^e instrument from 150 to 250°C with a heating rate of 10°C min^{-1} under nitrogen atmosphere (N_2 flow rate: 50 mL min^{-1}).

Fourier transform infrared-attenuated total reflection (FTIR-ATR)

Because of large thickness and flexible nature of membrane samples, it was unsuitable to use the IR test. Therefore, ATR-FTIR sampling technique was used to characterize PVdF/SPPESK blend membranes. Spectra of them were recorded on an EQUINOX 55 Fourier transport infrared spectrometer (BRUKER OPTICS) with a wave number range of 4000 cm^{-1} to 600 cm^{-1}, and the spectral resolution of 0.2 cm^{-1}.

Thermogravimetric analysis (TGA) and scanning electron microscope (SEM)

Thermal stability of samples was analyzed using thermogracimetric analysis (Mettler Toledo TGA/SDTA 851^e) from 100 to 800°C at a heating rate of 10°C min^{-1} under nitrogen atmosphere (N_2 flow rate: 50 mL min^{-1}). Before testing, the samples were dried for 2 h at 120°C in vacuum to remove moisture. Derivative thermogravimetry (DTG) curves were obtained from the first order differential of TGA curves on temperature. The morphology of the membranes was investigated using a scanning electron microscope (SEM) (KYKY-2800B). Samples were fractured in liquid N_2 and sputtered with thin layer of gold at vacuum before imaging.

Water uptake and swelling ratio

The membranes were immersed in deionized water at different temperatures for at least 10 h for full saturation. The liquid water on the surface of wet membranes was quickly removed with a dry filter paper, and then the weight and dimensions of the wet membranes were measured immediately. The weight and dimension of dry membranes were obtained after the wet membranes were dried for 24 h at 120°C in vacuum. The water uptake and swelling ratio can be calculated by the following equations:

$$\text{Water uptake} = \frac{W_{wet} - W_{dry}}{W_{dry}} \times 100\%$$

$$\text{Swelling ratio} = \frac{l_{wet} - l_{dry}}{l_{dry}} \times 100\%$$

where W_{wet} and W_{dry} are the weight of wet and dry membrane samples, respectively; l_{wet} and l_{dry} are the average length [$l_{wet} = (l_{wet1} \cdot l_{wet2})^{1/2}$, $l_{dry} = (l_{dry1} \cdot l_{dry2})^{1/2}$] of wet and dry samples, respectively, where, l_{wet1}, l_{wet2}, and l_{dry1}, l_{dry2} are the length and width of wet and dry membranes, respectively.[38]

Proton conductivity

Proton conductivity in transversal direction was measured using the two-electrode AC impedance spectroscopy method over the frequency range from 100 Hz to 1 MHz (EG and G Princeton potentiostat/Galvanostat 283A). Proton conductivity, σ, can be calculated using the following equation:

$$\sigma = L/[(R - r) \cdot A]$$

where L and A are the thickness of the membrane samples and electrode area (1 cm^2), respectively. R is derived from the low intersect of high frequency semicircle on the complex impedance plane with the Re(Z) axis, and r is the system internal resistance. During the measurement, the electrodes and membrane samples are immersed in deionized water at constant temperatures.

RESULTS AND DISCUSSION

XRD study

As a semicrystalline polymer, PVdF can form five crystal structures including four polar forms [I(β), II(α), IIIp(αp), and III(γp)], and one nonpolar form [III(γ)].[41] Seen in Figure 1, the PVdF diffraction peaks appear at 2θ = 18.3° (d-spacing (d) = 4.9 Å), 20.3° (d = 4.4 Å, form [I(β)]), and 38.8° (d = 2.3 Å, form [II(α)]). Only form [I(β)] diffraction peak can be found in PVdF/SPPESK blends with high PVdF content of 20–50%, and its intensity decreases with decreasing PVdF content. All above PVdF diffraction peaks are not found in the blends with low PVdF content of 5–15%, implying the good miscibility between PVdF and SPPESK. Also there is one weak diffraction peak found in pristine SPPESK locating at 2θ = 11.6° (d = 7.6 Å), and the corresponding crystalline size is 41.6 nm calculated by the Scherrer equation[42] below:

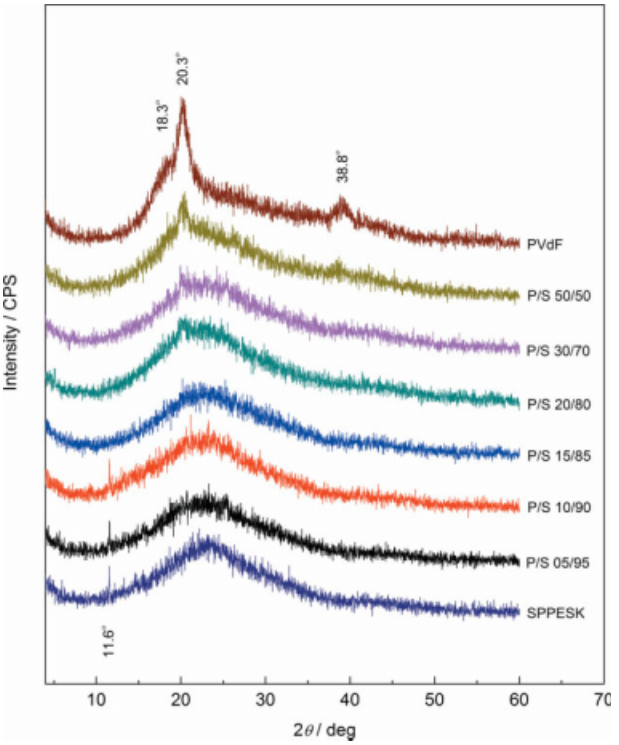

Figure 1 XRD patterns of PVdF, SPPESK, and PVdF/SPPESK blends. [Color figure can be viewed in the online issue, which is available at www.interscience.wiley.com.]

$$L = \frac{K\lambda}{W \cdot \cos\theta}$$

where K is the Scherrer constant (0.89), λ is the wavelength (1.5418 Å), W is the full-width radian at half-maxima of diffraction peak (0.003316, obtained from XRD pattern), and θ is the Bragg angle.

In terms of the blends, the SPPESK diffraction peak appears with low PVdF content of 5 and 10%, but disappears when PVdF content is equal or larger than 15%. Obviously, with increasing PVdF content, on one hand, SPPESK content decreases inevitably; on the other hand, the order of SPPESK polymer-chain is continuously disturbed by the introducing PVdF.

PVdF crystallinity

The DSC curves of PVdF, SPPESK, and PVdF/SPPESK blends are shown in Figure 2, and corresponding maximum endothermic temperatures, namely the melting points of PVdF crystals, T_m, are listed in Table I. The measured melting points (166–172°C) of PVdF in the blends are fairly close to that (170°C) in pristine membrane and no obvious trend with varying PVdF contents is observed here, which indicates the PVdF has the same/similar crystal-forming behavior in both the pristine membrane and

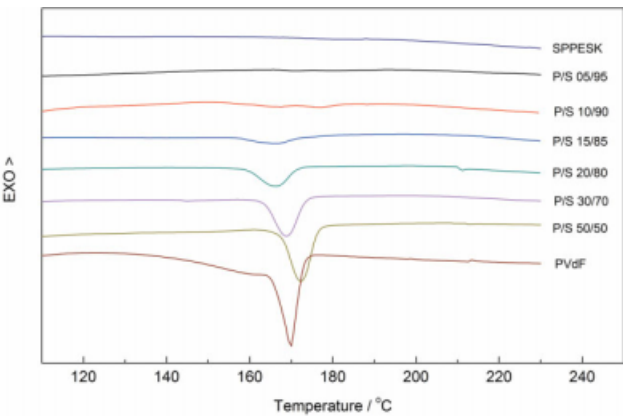

Figure 2 DSC curves of PVdF, SPPESK, and PVdF/SPPESK blends. [Color figure can be viewed in the online issue, which is available at www.interscience.wiley.com.]

the blends. Based on DSC curves, the PVdF crystallinity in pristine PVdF and PVdF/SPPESK blends can be calculated using the following equation:

$$\text{PVdF crystallinity} = \frac{\Delta H_f}{\Delta H_f^* \cdot C_{\text{PVdF}}} \times 100\%$$

where ΔH_f is the fusion heat of PVdF crystals derived from the area of endothermic peak in DSC curves and heating rate (ΔH_f = peak area/heating rate), ΔH_f^* is the fusion heat of perfect PVdF crystal (104.5 J g^{-1} [43]), and C_{PVdF} is PVdF content. ΔH_f and calculated PVdF crystallinity are also listed in Table I.

The PVdF crystallinity in PVdF/SPPESK blends depends on the PVdF content: initially, the PVdF crystallinity increases from 4 to 40% with PVdF content from 5 to 20%; and when PVdF content equals or larger than 20%, PVdF crystallinity levels off around 40% that identically equals to the PVdF crystallinity in pristine PVdF membrane. The reduced crystallinity reflects the good compatibility between the two polymers, especially with low PVdF content of 5–15%. When PVdF content reaches or exceeds

TABLE I
PVdF Crystallinity in PVdF/SPPESK Blend and Pristine PVdF Membranes

Sample	PVdF content (%)	Melting point (°C)	ΔH_f (J g^{-1})	PVdF crystallinity (%)
P/S 05/95	5	171	0.22	4
P/S 10/90	10	168	1.37	13
P/S 15/85	15	167	4.22	27
P/S 20/80	20	166	8.25	40
P/S 30/70	30	169	13.3	42
P/S 50/50	50	172	20.5	39
PVdF	100	170	42.0	40

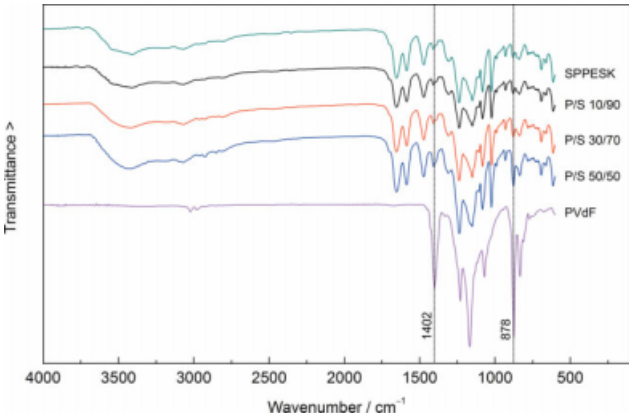

Figure 3 FTIR-ATR spectra of PVdF, SPPESK, and PVdF/SPPESK blends. [Color figure can be viewed in the online issue, which is available at www.interscience.wiley.com.]

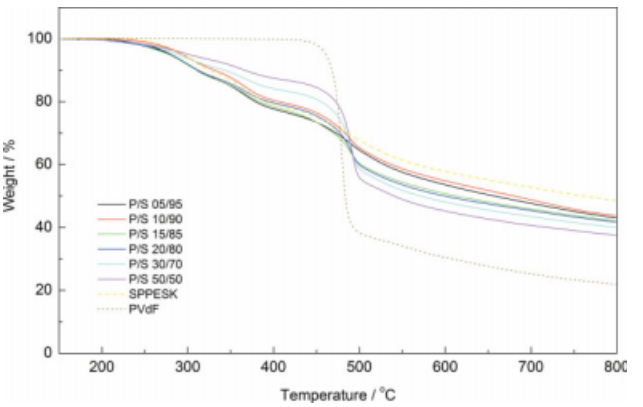

Figure 4 TGA curves of PVdF, SPPESK, and PVdF/SPPESK blends. [Color figure can be viewed in the online issue, which is available at www.interscience.wiley.com.]

20%, PVdF also can form the most crystals in the blends as in its pristine membrane.

FTIR-ATR spectra analysis

ATR spectra of PVdF, SPPESK, and PVdF/SPPESK blends are shown in Figure 3, and the assignment of ATR bands of PVdF[44–46] and SPPESK[38] are listed in Table II. ATR spectra of PVdF/SPPESK blends are much similar to that of SPPESK due to relatively strong absorption of SPPESK compared with PVdF. In terms of PVdF/SPPESK blends, the absorptions at 1402 cm^{-1} and 878 cm^{-1} (CH_2 wagging vibration and C—C—C asymmetrical stretching vibration of PVdF I(β), respectively), obviously increases with PVdF content. Whereas, the wave number and intensity of the characteristic absorptions (OH stretching at 3408 cm^{-1}, C=N stretching at 1587 cm^{-1}, SO_2 asymmetric and symmetric stretching in —SO_3H at 1084 and 1024 cm^{-1}, respectively) of SPPESK in PVdF/SPPESK blends are almost identical with those of pristine SPPESK, implying that there may not be strong atomic interaction between PVdF and SPPESK in the PVdF/SPPESK blends. Also, the intactness of —SO_3H in PVdF/SPPESK blends can also ensure the proton-conducting function.

TABLE II
Assignment of ATR Bands in PVdF and SPPESK

SPPESK Band (cm^{-1})	Assignment	PVdF Band (cm^{-1})	Assignment
3408	υ(OH) in —SO_3H	3023	$\upsilon_a(CH_2)$
1587	υ(C=N)	2980	$\upsilon_s(CH_2)$
1309	$\upsilon_a(SO_2)$ in main chain	1402	Iβ: ω(CH_2), υ_a(CCC)
1238	υ(COC)	1230	IIIγ: $\upsilon_a(CF_2)$, τ(CH_2), γ(CH_2)
1150	$\upsilon_s(SO_2)$ in main chain	1169	IIIγ: $\upsilon_s(CH_2)$, γ(CC), τ(CH_2)
1084	$\upsilon_a(SO_2)$ in —SO_3H	878	Iβ: υ_a(CCC), $\upsilon_a(CF_2)$
1024	$\upsilon_s(SO_2)$ in —SO_3H	834	Iβ: γ(CH_2), $\upsilon_a(CF_2)$
614	υ(CS)		

Thermal stability

The TGA and DTG curves of PVdF, SPPESK, and PVdF/SPPESK blends are shown in Figures 4 and 5, respectively. Corresponding onset decomposed temperatures ($T_{\text{d-onset}}$) and max weight-loss rate temperatures ($T_{\text{d-max}}$) are listed in Table III. PVdF has only one weight-loss step related to main-chain decomposition, and its $T_{\text{d-onset}}$ and $T_{\text{d-max}}$ are 470 and 480°C, respectively. SPPESK has three weight-loss steps (T_{d1}, T_{d2}, and T_{d3}): T_{d1} and T_{d2} are induced by two-step desulfonation where —SO_3H of SPPESK thermally collapses, and T_{d3} is attributed to main-chain decomposition. Here, the thermal stability of SPPESK is not identical to that we reported previously,[38] because SPPESK have been subjected to different solvent-removing processes (180°C for 5 h here and 120°C for 2 h in previous work). There are

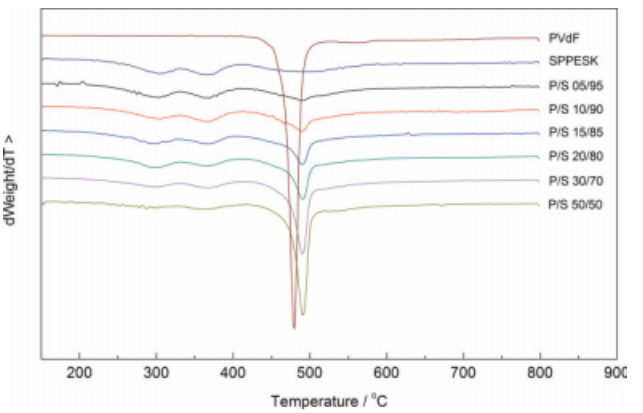

Figure 5 DTG curves of PVdF, SPPESK, and PVdF/SPPESK blends. [Color figure can be viewed in the online issue, which is available at www.interscience.wiley.com.]

TABLE III
Thermal Characteristic Temperatures of PVdF, SPPESK, and PVdF/SPPESK Blend Membranes

Sample	$T_{d1\text{-onset}}$ (°C)	$T_{d1\text{-max}}$ (°C)	$T_{d2\text{-onset}}$ (°C)	$T_{d2\text{-max}}$ (°C)	$T_{d3\text{-onset}}$ (°C)	$T_{d3\text{-max}}$ (°C)
P/S 05/95	255	302	349	367	458	492
P/S 10/90	261	305	349	363	462	490
P/S 15/85	250	298	350	368	468	490
P/S 20/80	253	298	350	365	471	490
P/S 30/70	246	297	349	363	474	490
P/S 50/50	247	295	345	363	477	492
PVdF	–	–	–	–	470	480
SPPESK	267	303	348	367	446	495

also three weight-loss steps (T_{d1}, T_{d2}, and T_{d3}) in PVdF/SPPESK blends. Obviously, T_{d1} and T_{d2} are related to the two-step desulfonation of SPPESK, and T_{d3} is related to mixed main-chain decomposition of PVdF and SPPESK, since they are fairly close to each other. From Table III, both $T_{d1\text{-onset}}$ (246–261°C) and $T_{d1\text{-max}}$ (295–305°C) of PVdF/SPPESK blends are all slightly lower than those of pristine SPPESK (267 and 303°C), indicating that the thermal stability of SPPESK slightly declines in PVdF/SPPESK blends possibly owing to the dipole–dipole interaction between the two polymers. Anyway, the thermal stability of PVdF/SPPESK blends is still very high and sufficient for PEM.

Morphology

SEM images of SPPESK and PVdF membranes are shown in Figure 6. The stick-like structure can be observed on the flat surface of SPPESK membrane, and some of them are irregular and congregating. Based on SPPESK XRD analysis aforementioned, these sticks could be related to the SPPESK crystal. From the cross section [Fig. 6(b)], the sticks inside membrane are far less than those on the surfaces, indicating that the SPPESK crystal may be prone to form on surface. Differently, PVdF membrane has a quite uneven surface [Fig. 6(c)] with many small spheres (related to PVdF IIIγ crystal[47]). Also, they

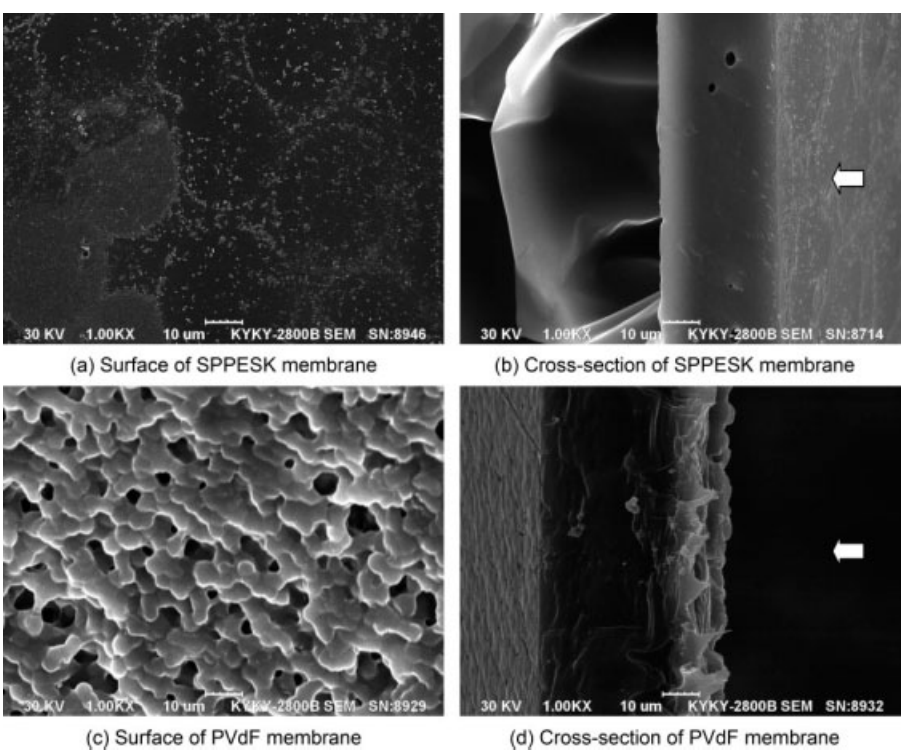

Figure 6 SEM micrographs of pristine PVdF membrane and pristine SPPESK membrane (×1000), the arrows pointing to the surface side.

only appear on surface [Fig. 6(d)], indicating that the surface surrounding (solvent evaporation, air contact) is the key factor to form this specific structure.

SEM images of PVdF/SPPESK blend membranes are shown in Figure 7. The surfaces of them show different morphologies. P/S 10/90 membrane has a flat surface, similar to SPPESK. On the contrary, the surfaces of P/S 20/80 and P/S 50/50 membranes are not even. Where some elliptic or circular pits emerge on surfaces of P/S 20/80 and P/S 50/50 membranes, and SPPESK sticks can also be found in the pits. One can speculate that the special pit structure should be related to the particular nature of blend of PVdF and SPPESK. The coarse surface may be an advantage to prepare membrane-electrode-assembly (MEA). The conformation of P/S 10/90 is more uniform and homogenous [Fig. 7(b)] than those of P/S 20/80 and P/S 50/50, which is well consistent with the PVdF crystallinity analysis in the earlier section, and demonstrates that with lower PVdF content, PVdF are very compatible with SPPESK.

Water uptake and swelling ratio

As expected, water uptake of PVdF/SPPESK blends increases with temperature and decreases with

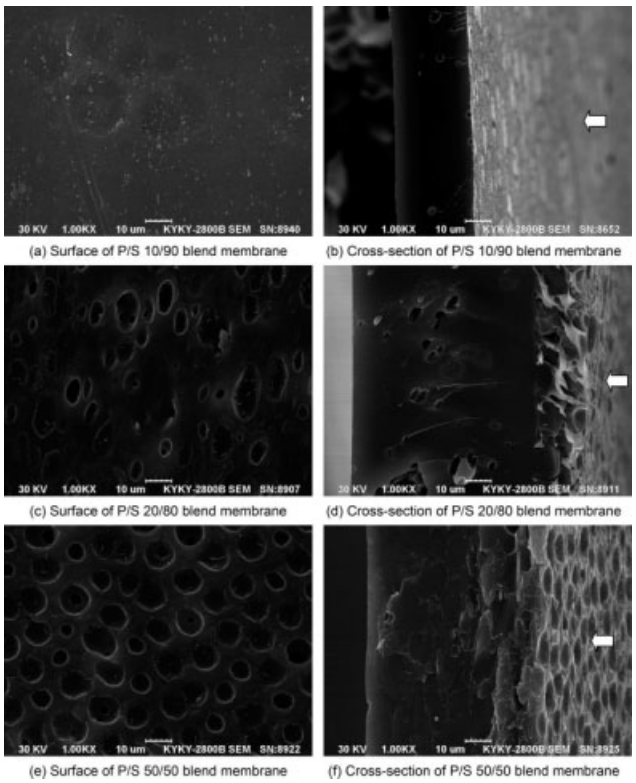

Figure 7 SEM micrographs of PVdF/SPPESK blend membranes (×1000), the arrows pointing to the surface side.

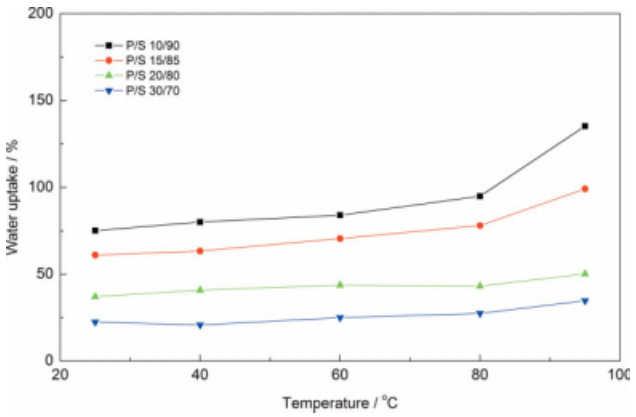

Figure 8 The effect of temperature on the water uptake of PVdF/SPPESK blend membranes. [Color figure can be viewed in the online issue, which is available at www.interscience.wiley.com.]

increasing PVdF content (Fig. 8). With lower PVdF content, the blends possess high water uptake, e.g., P/S 10/90 and P/S 15/85 have water uptake of 135 and 99% at 95°C, respectively. To further analyze water uptake, the average number of absorbed water molecules per sulfonic group (Λ) of PVdF/SPPESK blends are calculated using the following equation:

$$\Lambda = \frac{1000\,\mathrm{WU}}{18\,\mathrm{IEC}}$$

where WU is the water uptake and IEC is the ion exchange capacity. The calculated Λ as a function of temperature are plotted in Figure 9. Λ decreases remarkably with increasing PVdF content, showing that PVdF can strongly restrain water uptake. This reveals that the hydrophilic domains in the blends not only be compressed but also are divided by

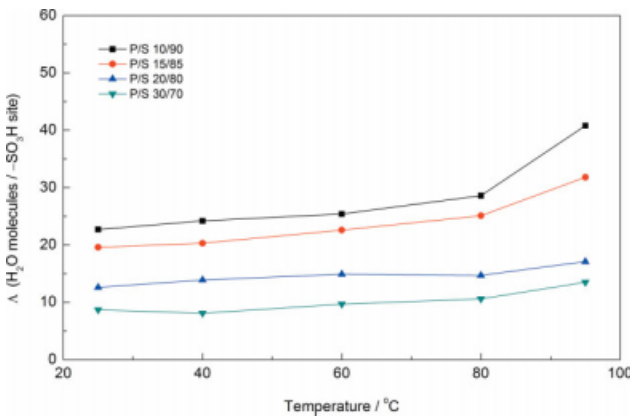

Figure 9 The effect of temperature on the average number of absorbed water molecules per sulfonic group of PVdF/SPPESK blend membranes. [Color figure can be viewed in the online issue, which is available at www.interscience.wiley.com.]

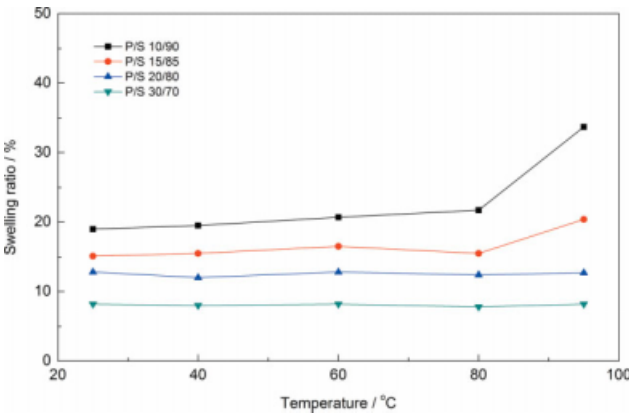

Figure 10 The effect of temperature on the swelling ratio of PVdF/SPPESK blend membranes. [Color figure can be viewed in the online issue, which is available at www.interscience.wiley.com.]

increasing hydrophobic PVdF. With PVdF content of 20% or 30%, Λ is low and has only a slight increment with temperature. Considering the PVdF crystallinity in the blends is as high as that in pristine PVdF aforementioned, one can suggest that PVdF could form a strong hydrophobic network to restrain combination and amplification of the hydrophilic domains in the blends. Having a similar trend, the effect of temperature on the swelling ratio of the blends is shown in Figure 10. Noticeably, temperature increment has no big influence on the swelling ratio with high PVdF content (20 and 30%), in agreement with the suggested strong hydrophobic PVdF network. The swelling ratios are at a fairly low level (e.g., 8–22%, 80°C), which shows the PVdF/SPPESK blend membranes have good dimension stability.

Proton conductivity

Proton conductivity (σ) of PVdF/SPPESK blend membranes decreases dramatically with increasing

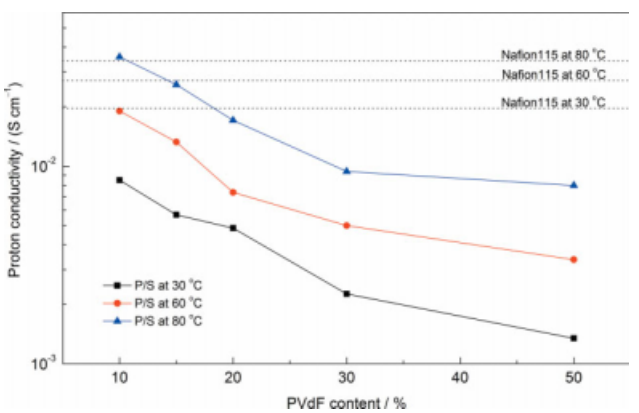

Figure 11 The effect of PVdF content on the proton conductivity of PVdF/SPPESK blend membranes. [Color figure can be viewed in the online issue, which is available at www.interscience.wiley.com.]

TABLE IV
Apparent Proton Migration Activation Energy of Proton Conductivity (ΔE_a) of PVdF/SPPESK Blend Membranes

Sample	ΔE_a (KJ mol^{-1})
P/S 10/90	25 ± 2
P/S 15/85	27 ± 2
P/S 20/80	21 ± 8
P/S 30/70	25 ± 2
P/S 50/50	31 ± 4
Nafion115	9.7 ± 0.6

PVdF content, as shown in Figure 11. The blends with lower PVdF content have high proton conductivity. As expected, proton conductivity is considerably enhanced by increasing temperature. Although proton conductivity of the blend membranes is less than that of Nafion at low temperature (e.g., 30°C), the blends with lower PVdF content (10 and 15%) have very high proton conductivity at elevated temperature, e.g., at 80°C, P/S 15/85 and P/S 10/90 blend membranes reach 2.6×10^{-2} and 3.6×10^{-2} S cm^{-1}, respectively, which are close or even higher to that (3.4×10^{-2} S cm^{-1}) of Nafion115 under the same test conditions. The temperature dependence of proton conductivity can be described by the Arrhenius relationship:

$$\ln\left[\frac{\sigma}{\mathrm{S\,cm^{-1}}}\right] = \ln\left[\frac{\sigma_0}{\mathrm{S\,cm^{-1}}}\right] - \frac{\Delta E_a}{RT}$$

where σ is the proton conductivity, σ_0 is the pre-exponential factor, ΔE_a is the apparent proton migration activation energy of proton conductivity, R is the universal gas constant (8.314 J K^{-1} mol^{-1}), and T is the temperature. The activation energy (ΔE_a) can be calculated from the slop of ln[σ/(S cm^{-1})] versus $1/T$. The calculated activity energies of PVdF/SPPESK blends and Nafion115 are listed in Table IV. The activity energies of the blend membranes are around 25 kJ mol^{-1} that is much higher than that (9.7 kJ mol^{-1}) of Nafion115. The possible reason is that the PVdF/SPPESK blend membranes have specific microstructure differently from that of Nafion. In addition, SPPESK has a significantly lower acidity, which may also play an important role in high value of ΔE_a.

CONCLUSIONS

PVdF/SPPESK blend membranes are successfully prepared by solution blending method. XRD and DSC analysis reveal that the PVdF crystallinity in the blends depends on PVdF content. The FTIR-ATR spectra indicate that SPPESK remains the proton-conducting function in the blends due to the

intactness of $-SO_3H$ group. Thermal analysis results show a very high thermal stability ($T_{d1} = 246$–$261^\circ C$) of the blends. PVdF crystallinity and morphology study demonstrate that with lower PVdF content, PVdF are very compatible with SPPESK. Also, with lower PVdF content, PVdF/SPPESK blend possess high water uptake, e.g., P/S 10/90 and P/S 15/85 have water uptake of 135 and 99% at 95°C. The blend membranes also have good dimension stability because the swelling ratios are at a fairly low level (e.g., 8–22%, 80°C). PVdF/SPPESK blends with low PVdF content exhibit very high proton conductivity at elevated temperature, e.g., at 80°C, P/S 15/85, and P/S 10/90 reaches 2.6×10^{-2} and 3.6×10^{-2} S cm^{-1} respectively, which are close to or even higher than that (3.4×10^{-2} S cm^{-1}) of Nafion115 under the same test conditions. All above properties indicate that the PVdF/SPPESK blend membranes (particularly, with 10–20% of PVdF content) are very promising for use in PEM field.

References

1. Gamburzev, S.; Appleby, A. J. J Power Sourc 2002, 107, 5.
2. Deluca, N. W.; Elabd, Y. A. J Polym Sci Part B: Polym Phys 2006, 44, 2201.
3. Alberti, G.; Casciola, M.; Massinelli, L.; Bauer, B. J Memb Sci 2001, 185, 73.
4. Yamaguchi, T.; Miyata, F.; Nakao, S. Adv Mater 2003, 15, 1198.
5. Jorissen, L.; Gogel, V.; Kerres, J.; Garche, J. J Power Sourc 2002, 105, 267.
6. Kerres, J.; Ullrich, A.; Hein, M.; Gogel, V.; Friedrich, K. A.; Jörissen, L. Fuel Cells 2004, 4, 105.
7. Yamada, M.; Honma, I. Electrochim Acta 2003, 48, 2411.
8. Nolte, R.; Ledjeff, K.; Bauer, M.; Mulhaupt, R. J Memb Sci 1993, 83, 211.
9. Kerres, J.; Cui, W.; Disson, R.; Neubrand, W. J Memb Sci 1998, 139, 211.
10. Mikhailenko, S. U. D.; Wang, K. P.; Kaliaguine, S.; Xing, P. X.; Robertson, G. P.; Guiver, M. D. J Memb Sci 2004, 233, 93.
11. Rhim, J. W.; Park, H. B.; Lee, C. S.; Jun, J. H.; Kim, D. S.; Lee, Y. M. J Memb Sci 2004, 238, 143.
12. Shiao, H. C.; Chua, D.; Lin, H. P.; Slane, S.; Salomon, M. J Power Sourc 2000, 87, 167.
13. Dang, Z. M.; Wu, J. B.; Fan, L. Z.; Nan, C. W. Chem Phys Lett 2003, 376, 389.
14. Ryu, H. S.; Ahn, H. J.; Kim, K. W.; Ahn, J. H.; Lee, J. Y. J Power Sourc 2006, 153, 360.
15. Flint, S. D.; Slade, R. C. T. Solid State Ionics 1997, 97, 299.
16. Lehtinen, T.; Sundholm, G.; Holmberg, S.; Sundholm, F.; Björnbom, P.; Bursell, M. Electrochim Acta 1998, 43, 1881.
17. Nasef, M. M.; Zubir, N. A.; Ismail, A. F.; Khayet, M.; Dahlan, K. Z. M.; Saidi, H.; Rohani, R.; Ngah, T. I. S.; Sulaiman, N. A. J Memb Sci 2006, 268, 96.
18. Martinelli, A.; Navarra, M. A.; Matic, A.; Panero, S.; Jacobsson, P.; Borjesson, L.; Scrosati, B. Electrochim Acta 2005, 50, 3992.
19. Peled, E.; Duvdevani, T.; Melman, A. Electrochem Solid State 1998, 1, 210.
20. Panero, S.; Ciuffa, F.; D'Epifano, A.; Scrosati, B. Electrochim Acta 2003, 48, 2009.
21. Shen, J.; Xi, J. Y.; Zhu, W. T.; Chen, L. Q.; Qiu, X. P. J Power Sourc 2006, 159, 894.
22. Bauduin, G.; Boutevin, B.; Gramain, P.; Malinova, A. Eur Polym J 1999, 35, 285.
23. Song, M. K.; Kim, Y. T.; Fenton, J. M.; Kunz, H. R.; Rhee, H. W. J Power Sourc 2003, 117, 14.
24. Cho, K. Y.; Eom, J. Y.; Jung, H. Y.; Choi, N. S.; Lee, Y. M.; Park, J. K.; Choi, J. H.; Park, K. W.; Sung, Y. E. Electrochim Acta 2004, 50, 583.
25. Tang, H. L.; Luo, Z. P.; Pan, M.; Jiang, S. P.; Liu, Z. C. J Chem Res 2005, 449.
26. Kim, H. J.; Kim, H. J.; Shul, Y. G.; Han, H. S. J Power Sourc 2004, 135, 66.
27. Chen, N. P.; Hong, L. Solid State Ionics 2002, 146, 377.
28. Prakash, G. K. S.; Smart, M. C.; Wang, Q. J.; Atti, A.; Pleynet, V.; Yang, B.; McGrath, K.; Olah, G. A.; Narayanan, S. R.; Chun, W.; Valdez, T.; Surampudi, S. J Fluorine Chem 2004, 125, 1217.
29. Chen, N. P.; Hong, L. Polymer 2004, 45, 2403.
30. Amarilla, J. M.; Rojas, R. M.; Rojo, J. M.; Cubillo, M. J.; Linares, A.; Acosta, J. L. Solid State Ionics 2000, 127, 133.
31. Rodriguez, S.; Linares, A.; Acosta, J. L. Macromol Mater Eng 2000, 283, 68.
32. Linares, A.; Acosta, J. L. Polym Int 2005, 54, 972.
33. Mokrini, A.; Huneault, M. A. J Power Sourc 2006, 154, 51.
34. Wootthikanokkhan, J.; Seeponkai, N. J Appl Polym Sci 2006, 102, 5941.
35. Xue, S.; Yin, G. P. Electrochim Acta 2006, 52, 847.
36. Wu, H. L.; Ma, C. C. M.; Kuan, H. C.; Wang, C. H.; Chen, C. Y.; Chiang, C. L. J Polym Sci Part B: Polym Phys 2006, 44, 565.
37. Gao, Y.; Robertson, G. P.; Guiver, M. D.; Ean, X. G.; Mikhailenko, S. D.; Wang, K. P.; Kaliaguine, S. J Memb Sci 2003, 227, 39.
38. Gu, S.; He, G. H.; Wu, X. M.; Li, C. N.; Liu, H. J.; Lin, C.; Li, X. C. J Memb Sci 2006, 281, 121.
39. Wu, X. M.; He, G. H.; Gu, S.; Chen, W.; Yao, P. J. J Appl Polym Sci 2007, 104, 1002.
40. Gu, S.; He, G. H.; Wu, X. M.; Guo, Y. J.; Liu, H. J.; Peng, L.; Xiao, G. K. J Memb Sci 2008, 312, 48.
41. Takakubo, M.; Teramura, K. J Polym Sci Part A: Polym Chem 1989, 27, 1897.
42. Virk, H. S.; Chandi, P. S.; Srivastava, A. K. Nucl Instrum Methods Phys Res B 2001, 183, 329.
43. Nakagawa, K.; Ishida, Y. J Polym Sci Part B: Polym Phys 1973, 11, 2153.
44. Peng, Y.; Wu, P. Y. Polymer 2004, 45, 5295.
45. Bachmann, M. A.; Koenig, J. L. J Chem Phys 1981, 74, 5896.
46. Kobayashi, M.; Tashiro, K.; Tadokoro, H. Macromolecules 1975, 8, 158.
47. Chen, N. P.; Hong, L. Polymer 2002, 43, 1429.